Icarus **147**, 292–300 (2000)
doi:10.1006/icar.2000.6425, available online at http://www.idealibrary.com on IDEAL®

Models of Radar Absorption in Europan Ice

John C. Moore

Arctic Centre, University of Lapland, Box 122, Rovaniemi 96101, Finland
E-mail: jmoore@levi.urova.fi

Received April 22, 1999; revised December 2, 1999

The detection of a sub-surface present-day ocean on Europa is of considerable interest. One possible method of detecting an ocean is by an orbiting radar sounder. The effects of a range of possible Europan ice chemistries on radar attenuation are investigated, using plausible Europa ice temperature profiles. Ice chemistries are derived from geochemical models of Europa predicting a sulfate-dominated ocean, a chloride-dominated ocean scaled from the Earth, and on experimental data on marine ice formed beneath ice shelves on Earth, on low-salinity sea ice and models of rock and ice mixtures. Chloride ions are expected to dominate the radar absorption because they are incorporated into the ice lattice, though if freezing rates are rapid or similar to sea ice, then brine pockets will dominate losses. In the case of an ocean being present underneath the ice, the range of attenuation found in the models is from about 5 dB/km for rock/ice mixtures up to 80 dB/km for sea ice models. However, perhaps the best model at present is for ice formed from a plausible sulfate-dominated ocean with the fraction of chloride incorporated into the ice set to the same as for low accretion rate Ronne Ice Shelf marine ice. This has a radar absorption of 9–16 dB/km for surface temperatures of 50–100 K. In the case of a convecting isothermal ice layer beneath a conducting ice lid, absorption in the conducting lid is lower for all the models than it is over an ocean as the convecting ice is modeled to be 250–260 K. Absorption in the isothermal layers is very high, but the interface between conducting and convecting ice may be marked by a reflection coefficient that enables it to be imaged. It is concluded that realistic ice-penetrating radars are likely to be able to penetrate some kilometers into the ice, though problems of interpretation caused by scattering are not considered here. © 2000 Academic Press

Key Words: **Europa; ices; radar; interiors; satellites.**

INTRODUCTION

Europa is known from spectroscopic and gravity data (Calvin *et al.* 1995, Anderson *et al.* 1998) to have a predominantly water ice crust, with a low density upper layer some 80–170 km thick that could be either ice or liquid water mixed with salts. The Galileo mission has provided significant evidence of a sub-surface ocean (Carr *et al.* 1998, Khurana *et al.* 1998). The surface of Europa shows little cratering, indicating a geologically young age; the detailed surface morphology is consistent with a rigid, relatively thin shell on a soft deeper layer. And magnetic field observations can be explained by induced fields generated by currents flowing in a salty, electrically conducting, liquid layer near the surface, all of which is consistent with a present-day ocean. Despite this circumstantial evidence, there is no clear-cut proof that an ocean still exists beneath the surface. One putative method of detecting an ocean, and for mapping the thickness variations of an ice cover above the ocean, is an orbital ice-penetrating radar.

The viability of the radar sounding technique depends on the ability of radar waves to penetrate the ice crust and on the returns being interpreted properly. Although the surface of Europa is quite smooth on large scales, the many ridges and chaotic ice regions exhibit very steep surfaces on scales smaller than kilometers (Carr *et al.* 1998). An orbiting radar has many problems associated with interpretation, mainly due to the large radar spot size on the satellite's surface and the corresponding extraneous clutter expected to come from reflection glints off steep ridges at large off-nadir angles. This problem may be more significant at the ice/liquid interface because the low Europan gravity and small density contrast between ice and water could lead to larger bottom topography than at the surface. The scattering problem, though significant, is susceptible to processing techniques. Here we will only consider the factors that govern the depth of penetration of radar waves into the ice, as this is a fundamental property of the ice itself.

In this paper we assume that the crust is composed of ice 1h, that is, the same ice phase as seen on Earth; which is consistent with the phase diagram of water under the geophysical conditions of Europa. Often (but not exclusively), we assume that the ice on Europa was derived from an ocean at some point in its the geological history. The models are not dependent on the current status of an ocean but are distinguished from scenarios where the ice is actually present in a mixture of rock and ice and has never suffered melting and freezing processes. This kind of ice is essentially that considered in the models of Chyba *et al.* (1998), and it is discussed here for comparison purposes. On Earth the naturally occurring ice types can be classified into three basic types: atmospheric precipitation that forms the glaciers and ice sheets, known as *meteoric ice*; ice formed by the freezing of water close to the atmospheric interface, typified by *sea ice*; and ice which forms beneath the large ice shelves of Antarctica from frazil ice crystals that form directly in the ocean water,

0019-1035/00 $35.00
Copyright © 2000 by Academic Press
All rights of reproduction in any form reserved.

called *marine ice*. Meteoric ice cannot be present on Europa in any quantity because of the lack of a significant atmosphere. Similarly sea ice is formed at the ocean–atmosphere interface on Earth; on Europa's surface, freezing and boiling would be very rapid, and the ice structure formed would be rather unlike sea ice. However, at an ice/ocean interface there is a good chance that processes similar to those on Earth would occur on Europa, suggesting that marine ice analogues are relevant. We will consider evidence on the radar properties of these types of ices in this study of plausible Europan ice composition.

RADAR ABSORPTION

Evans (1965) gives the attenuation rate of electromagnetic waves in ice,

$$\alpha = 0.129\sqrt{\varepsilon_\mathrm{r}}\, f\left[\sqrt{(1+\tan^2\delta)}-1\right]^{1/2}\,\mathrm{dB\,m^{-1}}, \tag{1}$$

where $\tan\delta = \varepsilon_\mathrm{i}/\varepsilon_\mathrm{r}$, ε_i and ε_r are the imaginary and real parts of the dielectric constant (permittivity), and f is the frequency in MHz. If $\tan\delta$ is $\ll 1$ (as it is for low loss materials such as most ice at radar sounding frequencies), this can be rewritten as

$$\alpha \approx 0.0009\sigma\ \mathrm{dB\,m^{-1}}, \tag{2}$$

where σ is the ice conductivity (in μS m^{-1}) appropriate for radar sounding frequencies. Comparison of electrical conductivity measurements on meteoric and laboratory ice at LF (about 100 kHz) with data from much higher radar and microwave frequencies suggests that there are no significant dielectric dispersions in the radar sounding range, and that ε_r does not vary with impurity concentration (Glen and Paren 1975, Moore and Fujita 1993). There is thus no change in the dielectric parameters of ice between the AF-range Debye dispersion, having a relaxation frequency that depends on impurity content and temperature (typically about 10 kHz), and the infrared absorption bands. This means that we can take data from the laboratory on the conductivity of ice made in the LF frequency range (typically at frequencies of 100 kHz to 1 MHz)—well above the Debye dispersion relaxation frequency—and apply them directly in radar absorption calculations.

The electrical conductivity of ice, and hence its absorption of radar waves, is dependent on the ice temperature and the nature and concentration of impurities it contains. Experiments on ice grown in laboratories, and on naturally occurring ices, have shown that the electrical conductivity of ice (which determines its dielectric loss and radar absorption coefficient) is governed by impurities that can be incorporated into the ice lattice, where they generate electrical defects (Gross *et al*. 1977, 1978, Glen and Paren 1975, Moore *et al*. 1992, 1994). Further radar losses come from interfacial polarizations and scattering that occur whenever the radar waves encounter material with different impedance. Important sources of loss in Earth sea ice are mm-scale brine pockets that are trapped in the ice. These give rise to Maxwell–Wagner interfacial polarizations that are strongly shape dependent, but which can be very large due to the large difference in dielectric constant between liquid brine and ice (typical dielectric constants of 86 and 3.2, respectively, Moore *et al*. 1992). The large number density of these small brine pockets accounts for much of the scattering loss in sea ice and has largely prevented use of radar as means of investigating sea ice thickness. The large loss factor also means that the condition of $\tan\delta \ll 1$ for Eq. (2) may not be fulfilled at 50 MHz.

Temperature Considerations

The temperature dependence of electrical conduction in ice has been typically approximated by an Arrhenius expression (Glen and Paren 1975). Corr *et al*. (1993) show that the electrical conductivity of ice, σ, can be expressed as a series of Arrhenius functions with impurity-specific activation energies and constants,

$$\sigma = \sum_{i=1}^{3} C_i \exp\left[\frac{E_i}{k}\left(\frac{1}{T}-\frac{1}{T_\mathrm{r}}\right)\right], \tag{3}$$

where T is absolute temperature and T_r is a reference temperature of 251 K. Here, C_i represents the conduction contribution from the various components in the ice, an intrinsic pure ice term amounting to 4.5 μS m^{-1} and the acid and chloride molar conductivities, which are 4 SM^{-1} for acids and 0.5 SM^{-1} for Cl^- at T_r (Moore and Fujita 1993); E_i is the species-specific activation energy; k is the Boltzmann constant. The activation energy for pure ice is rather high, about 0.6 eV or about 58 kJ/mol (Glen and Paren 1975), compared with those for impurities (Corr *et al*. 1992). This means that the relative importance of the pure ice term rapidly diminishes with decreasing temperature, while the effects of impurities dominate, leading to the activation energy of meteoric polar ice being typically close to 0.25 eV (24.2 kJ/mol) (Glen and Paren 1975). The activation energy for acid impurity is well known over the temperature range found in earth ice sheets, where acids are the dominant impurities, and it is about 0.25 eV. The activation energy for Cl^- from marine ice and meteoric ice is quite well known over a wide range of concentrations and at temperatures down to 210 K, and it is 0.19 eV (18.4 kJ/mol) (Moore *et al*. 1992).

The strong temperature dependence of σ in Eq. (3) means that the temperature profile in the Europan ice layer is a major factor in total radar absorption loss. Chyba *et al*. (1998) pay particular attention to the temperature profile in a conducting ice crust, which is probably governed both by the well-known surface and assumed basal temperatures and by the unknown distribution of tidal heating through the ice shell. Taking this into account, they give a temperature profile $T(z)$ as a function of depth from the surface,

$$T(z) = T_\mathrm{s}\exp(z/h), \tag{4}$$

where the surface temperature is T_s at $z = 0$ and $h = b/\ln(T_\mathrm{b}/T_\mathrm{s})$,

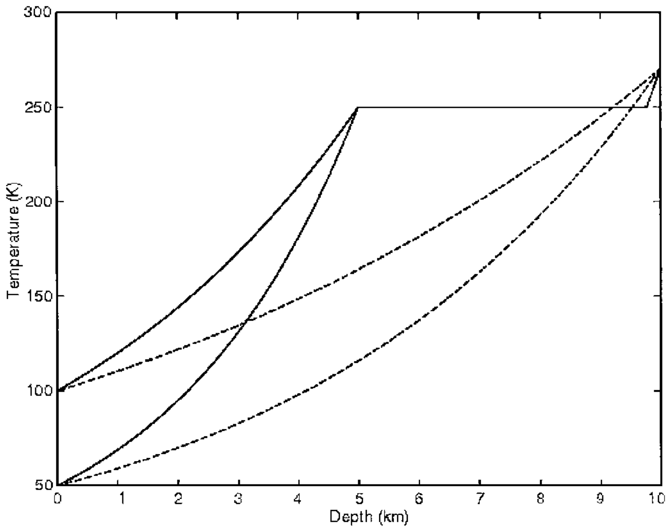

FIG. 1. Temperature distribution through a 10-km-thick ice crust given by Eq. (4), with surface temperatures of 100 and 50 K (dashed lines). The solid lines are for a 5-km-thick conducting lid overlying an isothermal convecting layer at 250 K with a lower conducting boundary.

where b is the ice thickness and T_b is the temperature at the ice base. The surface temperatures on Europa range from about 100 K at the equator to 50 K at the poles, and T_b is determined by the pressure melting point of ice. However, for Europa this is a minor effect and the basal temperature will be close to 270 K for reasonable ice thicknesses. We assume this form for the temperature profile in conduction-dominated ice since it considers ice rheology in the most realistic way to date. Several authors have proposed that an ice mantle on Europa will be likely to convect (Squyres *et al*. 1983, Pappalardo *et al*. 1998). Squyres *et al*. (1983) conclude that convection will rapidly cool and freeze any sub-surface ocean; conversely, McKinnon (1999) argues that the convecting shell will actually heat up, possibly leading to thermal instabilities and runaways leading to features such as diapirs. Pappalardo *et al*. (1998) use evidence from Galileo imagery to support the idea of convection under an rigid ice lid a few km thick. In the case of an isothermal convecting layer of ice, the value of T_b is taken to be the temperature of the isothermal layer rather than the ice base. Some profiles for purely conducting ice crusts and for a crust with an isothermal convecting layer are shown in Fig. 1.

POSSIBLE EUROPA OCEAN COMPOSITION

Kargel (1991) used a straightforward model of the geochemical evolution of Europa to deduce the composition of the upper icy crust. He expected the upper 110 km to be largely dominated by sulfate salts, mainly $MgSO_4$ and Na_2SO_4; however, there would also be about 1% by weight Cl, probably mainly NaCl and $MgCl_2$. All these salts are highly soluble in water, and any ocean of composition similar that predicted by Kargel (1991) will be hypersaline in sulfate salts. However, the chlorinity of such an ocean would be only about half that of Earth's ocean. Independent work based on the leachates obtained from meteorites of the carbonaceous chondrite type, thought to be representative of the original composition of Europa (Fanale *et al*. 1977, 1998), shows rather similar results—the salts in an icy crust or ocean on Europa will be dominated by magnesium and sodium sulfates, with additional quantities of $CaSO_4$. Another crude estimate of chlorinity of a Europan ocean, if processes similar to those on Earth occurred there, can be made by simply scaling the volume of H_2O relative to the crustal surface to which it is exposed on each body. If we take a thickness of 100 km of the ice/water crust of Europa, then its volume is rather similar to that of Earth's ocean, while the land surface of Earth is about 10 times Europa's surface area. So a simplistic estimate would be an ocean chlorinity about 1/10 that of Earth's oceans or about 3.5 ppt (salinity units in parts per thousand). However, this is likely to be a gross overestimate of the salinity of Europa's ocean due the lack of granitoid continental crust and considering that Europa has probably experienced no concentrated rates of weathering similar to those on the early Earth.

EUROPAN ICE COMPOSITION

At concentrations in the ice above a species-dependent solubility limit, the species must be present outside the crystal structure as a liquid or separate salt phase. The species that are known to have non-negligible solubility in ice are F^-, Cl^-, NH_4^+, and H^+ (Gross *et al*. 1978). Sulfate ions are not soluble in ice to any significant degree. Experiments on ice formed naturally on Earth, and in laboratories, show that SO_4^{2-} seems to play no role in electrical conduction, which is consistent with its insolubility, and with expectations considering the relative size of the oxygen and sulfate centers (Gross *et al*. 1978, Wolff *et al*. 1997). It is likely that ammonium salts play no part in Europan brine or ice formation, as temperatures in the nebula where Europa formed probably exceeded the condensation temperature for ammonium hydrate (Kargel 1991). However, if Jupiter and Europa formed much further away from the sun, then significant amounts of ammonia may be present, but we have little evidence to support this hypothesis at present. If large amounts of sulfate exist in any ocean on Europa, it may be possible that some H_2SO_4 may be present, which could contribute H^+ to the ice, and H_2SO_4 has been observed spectroscopically on some parts of the surface (Carlson *et al*. 1999). This acid is likely produced on the surface and may be transported deeper in the ice by the resurfacing process; however, the acid content of the deeper ice remains unknown. Carbonates are commonly seen in leachates from meteorites (Fanale *et al*. 1977) and also are consistent with spectroscopy observations of surface salts on Europa (McCord *et al*. 1998)—carbonates in an ocean would tend to neutralize acids and may even lead to alkaline water chemistry. F^- is cosmogenically rather rare. So we are left with Cl^- and possibly H^+ as the dominant soluble impurities in ice.

The solubility limit of Cl^- in ice as determined by laboratory experiments (Gross *et al.* 1977) on artificial ice, and on natural marine ice (Moore *et al.* 1994), is about 200–300 μM (0.01–0.02 ppt). Gross *et al.* (1977) give a distribution coefficient, $k = C_S/C_L = 3\times10^{-3}$, for the Cl^- concentration in ice relative to that in the liquid in which it is grown, based on laboratory experiments. Natural marine ice seems to have a lower k for Cl^- than laboratory grown ice. To a large degree the temperature gradient in the ice determines the incorporation of brine into ice. Sea ice typical forms in temperature gradients of order 10 K m^{-1}, while the marine ice beneath the Ronne Ice Shelf grew in much lower temperature gradients, of order 10^{-1} K m^{-1} (Oerter *et al.* 1992). The marine ice under the Ronne Ice Shelf seems to have formed from a mass of frazil ice crystals suspended in the water, which rise under the ice shelf to form a slushy layer on the order of 10 m thick, which slowly compresses and removes brine very efficiently. Slower rates of marine ice accumulation produce less saline ice (Moore *et al.* 1994).

THE ICE MODELS

In this paper we am interested in examining the range of possible radar absorptions that could be present in Europan ice. This ranges from basically pure ice to the sea ice type. The drawings in Fig. 2 illustrate several possibilities for ice formation and states. To calculate the various absorptions that may be given by

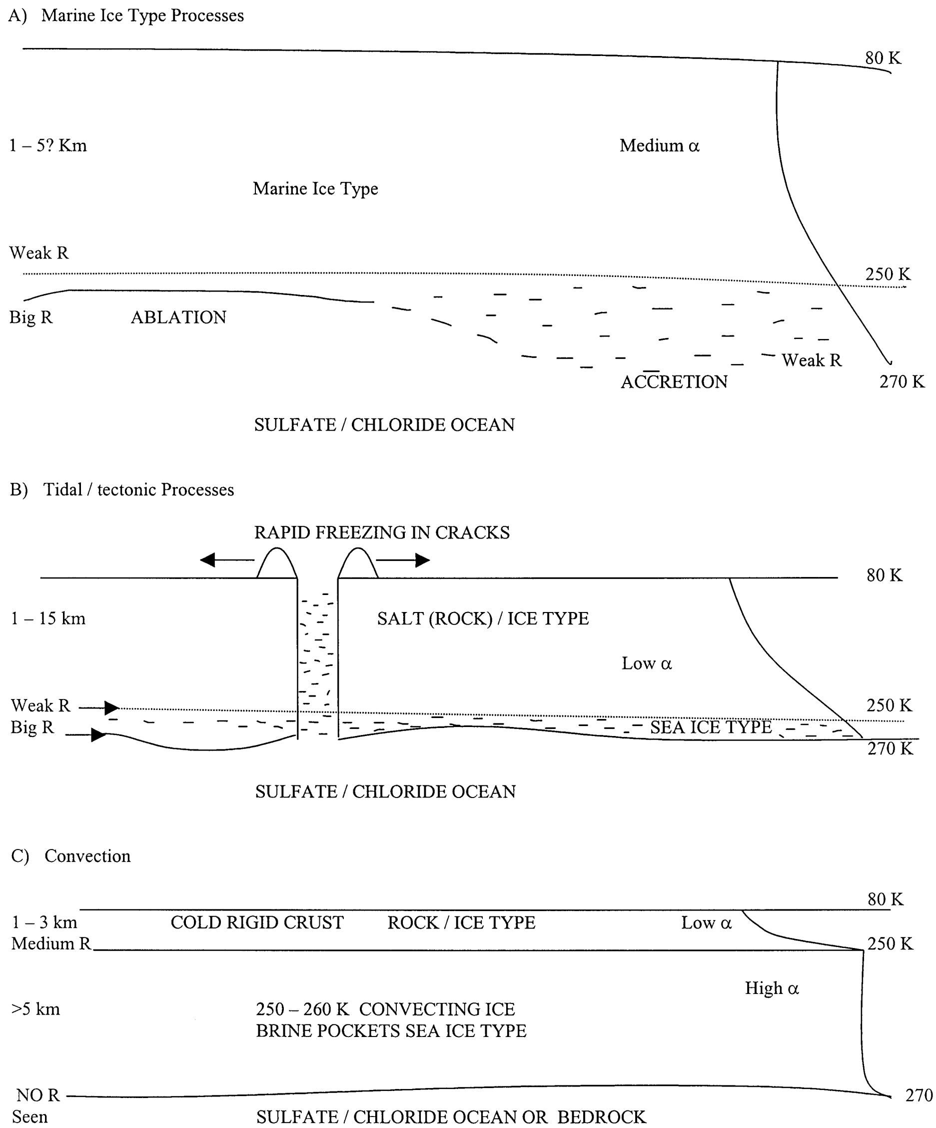

FIG. 2. Qualitative representations of ice types that may occur on Europa with radar absorption α and magnitude of radar reflection R at interfaces in the ice, illustrative temperature profiles (each assuming a "mid-latitude" surface temperature of 80 K), and ice thicknesses. (A) Processes that could occur if the ice is similar to Earth marine ice (e.g., Europa's chaotic terrains) with parts of the base subject to melting and others to accretion from frazil ice crystals. (B) Ice formation via extrusion into cracks or fissures (e.g., Europa's ridged plains), where rapid freeze-boiling occurs if an ocean is exposed to the surface conditions. (C) One possible convection scenario with a cold rigid lid underlain by thicker isothermal convecting ice.

TABLE I
Radar Absorptions for Various Ice Types and Temperatures

M	Ice type	Impurity content	α	I	II	III	Notes
0	pure ice	nil	0.0045	1.4–2.4	0.5–0.9	0.2–0.3	Glen and Paren (1975)
1	chloride-dominated Europa ice/ocean	3.5 ppt chlorinity ocean	0.016	4–7	2.5–4	1.6–2.8	Marine ice scaled from Earth ocean, $k_{\mathrm{MI}} = 7 \times 10^{-4}$
2	rock/ice	1% lunar soil	0.008	5–6	4–4.7	3.6–4.1	Chyba *et al*. (1998) recalculated
3	rock/ice	10% lunar soil	0.01	8–9	7–8	6–7	Chyba *et al*. (1998) recalculated
3	sulfate-dominated Europa ice/ocean	10 ppt chlorinity ocean	0.037	9–16	6–11	4–7	Kargel (1991); marine ice, $k_{\mathrm{MI}} = 7 \times 10^{-4}$
1	chloride-dominated Europa ice/ocean	3.5 ppt chlorinity ocean	0.05	14–24	10–17	7–12	Marine ice scaled from Earth ocean, $k_{\mathrm{O}} = 3 \times 10^{-3}$
1	rock/ice	50% lunar soil	0.021	30–33	29–32	28–31	Chyba *et al*. (1998) recalculated
2	depth-dependent Ronne Ice Shelf marine ice	0–400 μM Cl linear rise surface to bottom	varies	34–56	24–40	17–28	0–100% Ronne Ice Shelf ion content
2	sulfate-dominated Europa ice/ocean	10 ppt chlorinity ocean	0.15	36–61	25–44	18–31	Kargel (1991); marine ice, $k_{\mathrm{O}} = 3 \times 10^{-3}$
2	Ronne Ice Shelf marine ice	400 μM Cl (0.025 ppt salinity) ice	0.15	36–61	25–44	18–31	Moore *et al*.(1994) LF σ from core samples
0	Baltic Sea ice	ice grown in ≈3 ppt sea water	0.85 (at 270 K)	50–85	26–43	16–27	200 MHz radar measurement

Note. Attenuation, α, is in dB/m at 251 K. Columns I, II, and III are computed two-way attenuations, in dB/km, for ice shells with base temperatures of 270, 260, and 250 K, respectively. The range of values for each of these corresponds to surface temperatures of 50 and 100 K. These values are independent of shell thickness since the temperature profile is stretched to the ice thickness. The M column represents the plausibility of the ice type for Europa; 0 is least likely while 3 is more likely, given the present understanding of Europa. The distribution coefficients k_{O} and k_{MI} affecting the marine ice models come from laboratory experiments and Ronne Ice Shelf marine ice measurements, respectively.

the various models in Fig. 2, we need to calculate the absorptions of the various ice types under conditions likely to exist on Europa. For that we need the surface temperature, the temperature profile in the ice, and the chemical composition of the ice. Table I shows the relevant radar parameters for the various ices discussed in this paper. Since the radar absorption is governed by a dependence on temperature (Eq. (4)), which is exponential to a good approximation with depth, the two-way absorptions per km can be found for a given surface temperature independent of ice thickness. In Table I we take values 50 and 100 K as representative of the poles and the equator. Using the data in Table I it is then possible to calculate the radar absorptions for more "realistic" models of the ice simply by programming the layer depth and temperature ranges for each type of ice.

As an end member in this study we will take the case of sea ice formed in the relatively low salinity Bay of Bothnia in the Baltic Sea, where water salinities are about 3 ppt. The ice fabric is of the sea ice type and brine pockets are common, with ice salinities of about 0.5–1 ppt (Weeks *et al*. 1990). The data were measured *in situ* using a 200 MHz radar system at about 270 K; the activation energy was taken to be 0.6 eV (58 kJ/mol) between 270 and 250 K and 0.19 eV (18.4 kJ/mol) at colder temperatures. The choice of activation energy is poorly constrained since there are few data on sea ice characteristics at temperatures below those experienced *in situ* on Earth. However, data from artificial sea ice (Addison 1975) showed that changes in dielectric behavior at the eutectic points of various salts occurred, and that liquid brine effects dominate the response at temperatures warmer than about 220 K. Kovacs *et al*. (1987) present a model of radar attenuation in undeformed sea ice that exhibits very high activation energies at temperatures above 245 K, which are also consistent with the importance of liquid brine inclusions playing the dominant role at warm temperatures. The activation energies and absorption values chosen here are reasonably consistent with Kovacs *et al*. (1987) and Addision (1975), and with marine ice at 251 K containing Cl^- at the solubility limit. Despite the very low solubility limit of SO_4^{2-} there appear to be no liquid brine pockets visible in marine ice containing less Cl^- than its solubility limit (Moore *et al*. 1994). This may be because SO_4^{2-} is relatively low in concentration in marine ice, so any brine pockets that do exist are rare, small, and undetected, or because the non-Cl^- ions are not present in a liquid form but may be isolated at grain boundaries or in interstitial spaces in the crystal structure. If a similar mechanism occurs on Europa, and if the chloride concentration is below the solubility limit, then there may be no liquid brine pockets in the ice.

For the sake of completeness we include the pure ice absorption here as an end member of the range of possible absorption models. We select the pure ice conductivity and activation energy from Glen and Paren (1975), since it has the highest activation energy reported and probably represents the most pure ice sample measured.

A more realistic end member comes from Chyba *et al*. (1998), who modeled the icy shell of Europa as 1, 10, and 50% lunar soil mixed with pure ice, with the 1% mixture taken as a more plausible end member than pure ice. We have recalculated the absorption losses for these models using the pure ice behavior described above. This leads to small differences from the losses given in Chyba *et al*. (1998). The mixtures contribute to absorption through the differences in permittivity between pure ice and the rock components, using a Rayleigh mixing formula for spherical scattering bodies in a background medium. No soluble impurities are considered. This type of model could represent a Europan ice crust that had been well below the melting point throughout its history, or it could represent the ice formed if ice and salts were formed in the cracks and then spread over much of the crust (Fig. 2B). If the ice is convecting with a cold brittle lid underlain by warmer ice at perhaps 235–260 K (Pappalardo *et al*. 1998, Chyba *et al*. 1998, McKinnon 1999), then the cold lid would have a similar response, since the permittivity of solid salts is similar to that of rock. However, the deeper warm layer is likely to contain brine pockets as the ice temperature will be above the eutectic point of some chloride salts (Kargel 1996). In this case radar absorption will become very high—similar to that in the Baltic Sea or even higher (Fig. 2C). If the boundary is reasonably sharp, there will be a radar reflection from it due the change in dielectric impedance. The magnitude of the reflection will depend on the brine content in the ice. For example, that observed at the boundary between cold–dry and temperate–wet ice in polythermal glaciers is typically about −20 dB (Bamber 1987), a significantly smaller reflection than that from an abrupt ice/ocean interface.

As an example of the calculation method used in general, we shall illustrate the method by describing the process shown in Fig. 2B in some detail, assuming some parameters that are consistent with the model—though these are quite arbitrary. We shall assume that the total ice thickness is 5 km, and the temperature distribution is given by Eq. (4), with a surface temperature of 80 K chosen to represent a typical surface state. The rock/salt ice composition is a 1% mixture of NaCl in pure ice. Below depths where the temperature is greater than the NaCl eutectic point (250 K), we assume that the ice behaves like old sea ice; i.e., the salt has tended to drain out until salinities are rather like those of Baltic Sea ice, (about 1 ppt, or 0.1%). Then we set up a calculation of the absorption in a series of 1-m-thick layers each with a temperature from Eq. (4) and with contributions to conductivity given by Eq. (3), the components in Eq. (3) at 251 K being 4.5 μS m^{-1} (0.0045 dB/km) for pure ice and 2.3 μS m^{-1} for 1% rock/ice, with activation energies of 0.6 and 0.0025 eV, respectively. Then ice below the 250 K layer having the Baltic Sea ice conductivity of 140 μS m^{-1} (at 251 K) and an activation energy of 0.6 eV is used instead of the chloride component until the base of the ice is reached at 270 K. The total radar losses are then calculated from the conductivities of each layer using Eq. (2). Figure 3 shows the absorption loss as a function of depth for the particular parameters chosen for this run of the model. Note the sharp increase in absorption at the transition from solid-phase electrical conduction via defects in the ice lattice below 250 K to conduction via brine inclusions above 250 K. Although the total absorption in the ice is more than 250 dB, the absorption is well below 30 dB at the 250 K interface.

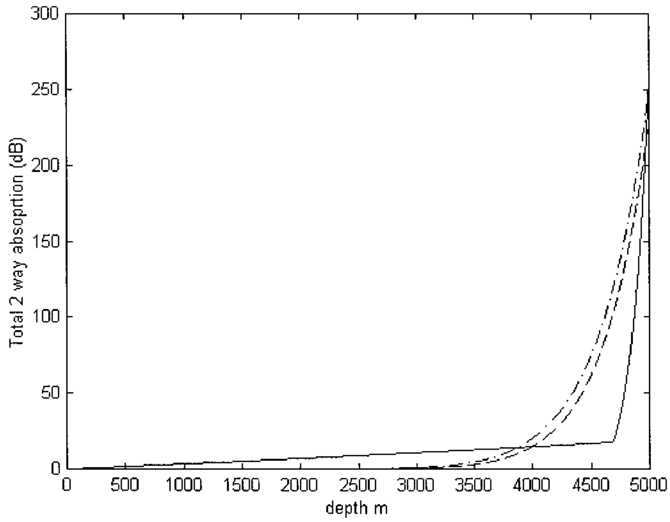

FIG. 3. Total two-way attenuation due to ice conduction for the models illustrated in Fig. 2. The surface temperature is 80 K and total ice thickness is 5 km in each of the models. The solid line represents the one realization of the absorption model shown in Fig. 2B. The upper layer of ice is 1% salt/ice mixture, while the lower layer at $T > 250$ K is of Baltic Sea ice type. The dot-dashed curve represents a model of type 2A, where the ice is of Ronne Ice Shelf type (or sulfate-dominated model ocean derived Europa ice). The dashed curve is also Ronne Ice Shelf ice but with a variable ionic impurity concentration that varies from zero at the surface to 100% of that of the Ronne Ice Shelf at the base.

It is also significant that this relatively abrupt change in conductivity will lead to a radar amplitude reflection coefficient that we can approximate by assuming a step change across a sharp boundary between two semi-infinite slabs, $r \approx 1/2\Delta \tan\delta = 1/2\Delta\sigma/(2\pi f \varepsilon_r \varepsilon_0)$ (ε_0 is the permittivity of free space, 8.854×10^{-12} F m^{-1}), giving r of about 0.01 (about −40 dB). The introduction of brine in the ice will also change the ice permittivity significantly, as the relative permittivity of brine is about 90 while for ice it is about 3. A typical Baltic Sea ice permittivity at 50 MHz is about 4; we could therefore expect an amplitude reflection coefficient, $r \approx 1/2\Delta\varepsilon_r/\varepsilon_r$, corresponding to a power reflection of about −20 dB.

Figure 2A illustrates a marine ice Europan crust, with parts subject to bottom melting and others to accretion. The experimental values of conductivity obtained on Ronne Ice Shelf marine ice are well known at LF over the temperature range 0–70°C (Moore *et al*. 1994). Table I gives the calculated absorption losses for this ice. To calculate the absorption losses of marine ice models, it is necessary to estimate the distribution coefficient k. Gross *et al*. (1977) give the value $k_O = 3 \times 10^{-3}$, based on laboratory experiments. However, it is clear that somewhat lower distribution coefficients must have created the lowest salinity marine ice samples recovered from beneath the Ronne Ice Shelf, which give $k_{MI} = 7 \times 10^{-4}$ (Moore *et al*. 1994). As discussed earlier, the value of k depends on the nature of the freezing conditions, which are poorly known for terrestrial marine ice but certainly include the temperature gradients and currents in the water around the crystals. The desalination process that occurs in the mush of frazil ice crystals is critical, and the effects of lower gravity on a possible Europan mush of ice crystals would act to delay compaction. This probably allows more efficient brine removal from the mush, and the eventual marine ice, than would occur under Earth gravity. The lowest salinity marine ice samples are those that formed under the slowest accretion rates, and k_{MI} may therefore be more representative of the value of k appropriate for a putative Europan ice accretion process than the k_O found from the laboratory experiments. At temperatures warmer than the salt eutectic points, brine pockets could occur, but given the low chlorinity of the modeled oceans, they may not occur in Europan ice, as the Cl^- ice concentration would be lower than the solubility limit.

It can be postulated, as a variation on the models discussed so far, that the ionic concentrations in a particular ice type could vary with depth, especially if basal freezing of ice from an ocean is taking place, with the deeper ice having larger ion concentrations than the near surface. This is consistent with the Earth-based radar scattering experiments showing that surface ice has very low loss—though this would be a consequence of the low temperatures for any relatively clean ice. To investigate increasing ion concentration with depth, we selected a marine ice type with a chloride concentration varying linearly between zero at the surface and that of Ronne Ice Shelf marine ice at the bottom. Again, as the temperature profile is exponential the behavior can be represented as absorption/km of ice independent of the ice thickness, and also independent of the functional form of the ion depth relation (providing the function is reasonably smooth). The model is presented in Table I. Note that the absorption per km is somewhat lower than that for the uniform Ronne Ice Shelf ice, though not by much as the ions are concentrated in the warmer ice near the bottom, where the majority of the absorption takes place. However, this does mean that the radar would penetrate a deeper fraction of the total ice layer, as the absorption would rise much more steeply near the bottom than if the ice had uniform impurity distribution. This is illustrated by the curves in Fig. 3.

Figure 4 shows the radar absoprtion for 1 km of ice as a function of depth for the 1 and 10% rock/ice mixes and the sulfate-dominated Europa ocean marine ice models. We choose a 1-km thickness purely to illustrate how absorption varies through the ice thickness, and thus how well it may be expected to return echoes. For example if the ice were actually 5 km thick the absorption curves would look identical except scaled by a factor of 5, as from Table I it is the absorption *per km* that is actually calculated for each of the models. Figure 2 shows three proposed ice formation processes on Europa. Note that for both the "marine ice" (A) and the "tidal/tectonic" (B) examples, a reasonably smooth ice/ocean interface with properties derived from the non-sea-ice entries of Table I (i.e., a reflection coefficient of about −3 dB) can be well characterized, given a reasonable radar dynamic range of 50 dB. In addition, the reduced reflection strength from ice–rock/sea–ice interfaces (e.g., a reflection coefficient of

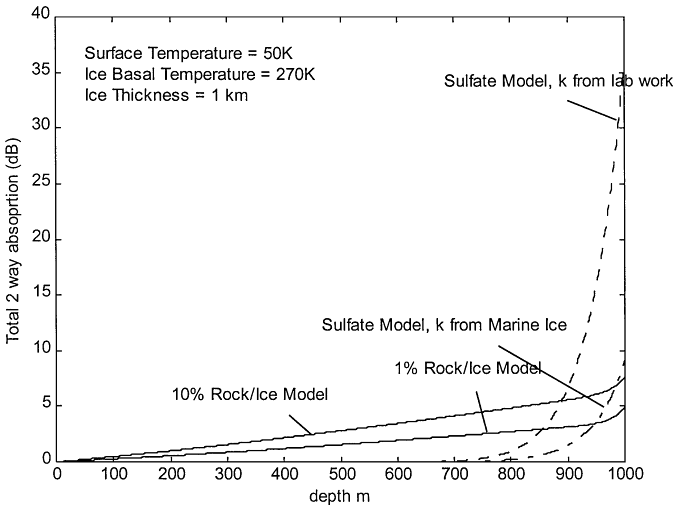

FIG. 4. Total two-way attenuation due to ice conduction for some of the ice types in Table I, for ice of 1 km thickness and a surface temperature of 50 K. For larger ice thicknesses the depth would scale the total absorption, as would the fractional absorption at any depth. Ronne Ice Shelf marine ice and the sulfate-dominated Europa ocean model with k_O have the same absoprtion characteristics; the curves for 10% rock/ice mixtures and the sulfate ocean model with k_{MI} have similar total absorption but different losses with depth because of their very different activation energies.

about −20 dB) should still allow the base of the rigid ice lid in the convection model (C) to be detected and characterized. A final important result is that the negligible absorption for the upper 80% of the non-isothermal ice for all three models (Fig. 4) could allow even very weakly reflecting geophysical interfaces to be imaged.

Finally we consider the case where a conducting rigid ice lid lies on top of a convecting lower layer of ice. This type of structure has been proposed for many years (e.g., Ojakangas and Stevenson 1989, McKinnon 1999) and has been used to explain some of the geological features of Europa (Pappalardo *et al.* 1998, McKinnon 1999). Chyba *et al.* (1998) give a temperature profile in a simple convecting thermal model for Europa. The essential elements are a conducting lid, an isothermal convecting part at some temperature taken to be between 235 and 250 K, and a lower conducting boundary layer. McKinnon (1999) suggests a temperature of 260 K for the convecting layer. The ice shells in convecting models tend to be quite thick, at least 5 km with a more likely limit closer to 20 km. If ammonia is present in the ice, a eutectic point closer to 200 K could be reached, leaving the possibility of much lower temperature convention. We investigated the absorption loss, as a function of ice depth, for conducting lids and for convecting layers of 2, 5, and 8 km for convecting layer temperatures of 250 and 260 K in a 10-km total ice thickness model. Temperature profiles for all layers were based on Chyba *et al.* (1998) (Fig. 1). For the "convection" processes of Fig. 2, the deeper warm layer is likely to contain brine pockets as the ice temperature will be above the eutectic point of some chloride salts (and ammonium salts—which also have roughly twice the molar conductivity of chloride salts at low concentrations without brine being present; Wolff *et al*. 1997). Because of this, absorption will become very high (similar to the sea ice of the Baltic Sea or even higher; Table I) and radar will be unable to penetrate the ice to any sub-surface ocean. In the case of ammonia ice convention at lower temperatures, penetration will be greater, but the effects of liquid inclusions will still be severe. However, it is possible that radar will penetrate the upper lid and reach the convecting layer beneath. This can be modeled as earlier, but taking the basal ice temperature as that of the convecting layer. The results are again presented as two absorption losses per km in Table I, but this is the absorption to the interface. The details of the interface are poorly constrained by theory at present, though it is likely, given the large differences in surface features of Europa (chaos areas and ridged plains), that the convecting interface could be very inhomogeneous. If the boundary is reasonably sharp, there will be a radar reflection from it due to the change in dielectric impedance. The magnitude of the reflection will depend on the brine content in the ice and its spatial distribution. A relevant example is the reflection coefficient observed at the boundary between cold–dry and temperate–wet glacier ice with an essentially uniform distribution of water pockets, which is typically about −20 dB (Bamber 1987). Assuming a similar reflection coefficient for convection processes on Europa (Table I and Fig. 2) shows that it is very likely that radar will penetrate the full range of expected rigid lid thicknesses and allow characterization of the interface with the convecting layer beneath.

IMPLICATIONS FOR FUTURE SPACE MISSIONS

Chyba *et al*. (1998) suggest a typical radar for Europa may be expected to have at least a detection limit of 50 dB, which could potentially be increased to 80 dB using processing techniques. The range of absorption losses for plausible Europan ices is quite large. Perhaps the most likely ice type (assuming that there is an ocean) would be the sulfate-dominated ocean with a marine ice distribution coefficient, giving 9–16 dB/km losses. This model is based on plausible geochemical models of Europan evolution and observed values of the rate of chloride ion incorporation into marine ice. The absoprtion losses of this type of ice are about midway in the range of absorption losses. The chloride-dominated oceans are unlikely based on the current understanding of Europan geochemistry. Ice with 50% rock is not supported by spectroscopic observations. Higher absorption rates given by ice types containing more impurities due to higher distribution coefficients may occur, but terrestrial marine ice has a lower distribution coefficient. Table I shows that ice thicknesses of between 1 and 10 km will probably be penetrated on the basis of ice types similar to terrestrial marine ice without brine pockets. If the ice is more like sea ice (that is, with brine pockets), penetration will be highly problematic, as an ice cover as thin as 1 km would likely give a bottom return obscured by surface clutter.

In assessing the probable behavior of a Europa radar to detect interfaces within ice it would be useful to compare its performance using terrestrial analogies. The wet/dry contacts typical of polythermal glaciers will be of direct usefulness in assessing radar performance. Tests over these glaciers, which are found fairly widely for the Arctic regions (especially Svalbard and in parts of the Canadian Arctic), will be helpful to observe high-angle contacts between wet and dry ice—which are formed in polythermal glaciers by the wetting of ice via crevasse zones, but which could model features such as cryo-volcanism on Europa.

The contact between fresh meteoric ice and slightly saline marine ice provides a strong dielectric boundary between ice types that is continuous over tens of kilometers on the Ronne Ice Shelf. The contrast in ice properties at the interface between the upper meteoric ice and the lower marine ice may be somewhat typical of ice containing small levels of brine (as seen in marine ice), which could with certain geochemistries be present on Europa. The contact is, however, generally horizontal, having been formed by bottom freezing on an ice shelf with only slowly varying topography. Thus it lacks the high angle contacts that seem probable from the imagery of the surface features.

A thick convecting layer of warm ice is unlikely to be penetrated due to the probable presence of brine pockets in the ice. However, it is likely that the contrast at the cold ice/temperate ice boundary will be easily detected and distinguishable from that between ice and ocean. The relative amounts of ice (if any) produced by surface fracturing, rapid freezing, and then burial and the ice formed by bottom freezing are probably variable on Europa; indeed the ice could have been formed by other mechanisms entirely. The radar response is thus likely to be quite varied, but calculations of radar absorption and reflection coefficients will help to provide clues on the formation and distribution of ice types on Europa, and the underlying ocean chemistry.

CONCLUSION

The importance of the radar absorption of Europa ice has been illustrated in this paper. It is clearly not sufficient to assume simple mixtures of rock and ice, or to assume the terrestrial meteoric ice behavior is valid for Europa, especially if an ocean exists beneath the ice. The calculation of the radar absorption of the Europa ice layer is rather poorly constrained at present. Several methods exist for refining this calculation. Laboratory experiments to determine the radar properties of salts and also acids over the temperature ranges from liquid nitrogen to melting point are needed (e.g., Lorenz 1998), especially for the kinds of ices that are formed from hyper-saline waters. Here, “saline” includes chlorides, sulfates (including sulfuric acid), and even ammonium salts. The radar investigation of Europa offers an excellent chance of determining the sub-surface structure of Europa to depths of several km, or at least to the first geophysically significant interface—whether that is an ocean, a convecting ice layer, or a layer of differing physical-chemical composition. The interpretation of radar returns from Europa will be a non-trivial problem that could be examined by several terrestrial analogues involving interfaces between ices of varying liquid and chemical compositions. The fact that radar on terrestrial glaciers and ice sheets is so widely used and is such a generally successful tool suggests that it could have valuable applications on the icy bodies of the Solar System, and especially the relatively "clean" ice of Europa.

ACKNOWLEDGMENTS

Discussions with T. V. Johnson, C. Chyba, F. P. Fanale, and J. S. Kargel and the two excellent anonymous reviews were invaluable in preparing this paper.

REFERENCES

Addison, J. R. 1975. Electrical properties of saline ice at 1 kHz down to $-150°$C. *J. Appl. Phys*. **46**, 513–522.

Anderson, J. D., G. Schubert, R. A. Jacobson, E. L. Lau, W. B. Moore, and W. L. Sjorgren 1998. Europa's differentiated internal structure: Inferences from four Galileo encounters. *Science* **281**, 2019–2022.

Bamber, J. L. 1987. Internal reflecting horizons in Spitzbergen glaciers. *Ann. Glaciol.* **9**, 5–10.

Calvin, W. M., R. N. Clark, R. H. Brown, and J. R. Spencer 1995. Spectra of the icy Galilean satellites from 0.2 to 5 μm: A compilation, new observations, and a recent summary. *J. Geophys. Res.* **100**, 19041–19048.

Carlson, R. W., R. E. Johnson, and M. S. Anderson 1999. Sulfuric acid on Europa and the radiolytic sulfur cycle. *Science* **286**, 97–99.

Carr, M. H., M. J. S. Belton, C. R. Chapman, M. E. Davies, P. Geissler, R. Greenberg, A. S. McEwen, B. R. Tufts, R. Greeley, R. Sullivan, J. W. Head, R. T. Pappalardo, K. P. Klaasen, T. V. Johnson, J. Kaufman, D. Senske, J. Moore, G. Neukum, G. Schubert, J. A. Burns, P. Thomas, and J. Veverka 1998. Evidence for a subsurface ocean on Europa. *Nature* **391** 363–365.

Corr, H. F., J. C. Moore, and K. W. Nicholls 1993. Radar absorption due to impurities in Antarctic ice. *Geophys. Res. Lett*. **20**, 1071–1074.

Chyba, C. F., S. J. Ostro, and B. C. Edwards 1998. Radar detectability of a subsurface ocean on Europa. *Icarus* **134**, 292–302.

Evans, S. 1965. Dielectric properties of ice and snow—A review. *J. Glaciol*. **5**, 773–792.

Fanele, F. P., T. V. Johnson, and D. L. Matson 1977. Io's surface and the histories of the Galilean satellites. In *Planetary Satellites* (J. Burns, Ed.), pp. 379–405. Univ. of Arizona Press, Tucson.

Fanale, F. P, Y.-H. Li, E. Decarlo, N. Domergue-Schmidt, S. K. Sharma, J. C. Granahan, and the Galileo NIMS team 1998. Laboratory simulation of the chemical evolution of Europa's aqueous phase (abstract), CDROM, *Lunar and Planet Sci*. **XXIX** (1248). Lunar and Planetary Institute, Houston.

Geissler P. E., R. Greenberg, G. Hoppa, P. Helfenstein, A. McEwen, R. Pappalardo, R. Tufts, M. Ockert-Bell, R. Sullivan, R. Greeley, M. J. S. Belton, T. Denk, B. Clark, J. Burns, J. Veverka, and the Galileo Imaging Team 1998. Evidence for non-synchronous rotation of Europa. *Nature* **391**, 368–370.

Geissler, P. E., R. Greenberg, G. Hoppa, A. McEwen, R. Tufts, C. Phillips, B. Clark, M. Ockert-Bell, P. Helfenstein, J. Burns, J. Veverka, R. Sullivan, R. Greeley, R. T. Pappalardo, J. W. Head III, M. J. S. Belton, and T. Denk 1998. Evolution of lineaments on Europa: Clues from Galileo multispectral imaging observations. *Icarus* **135**, 107–126.

Glen, J. W., and J. G. Paren 1975. The electrical properties of snow and ice. *J. Glaciol*. **15**, 15–37.

Gross, G. W, I. Cox Hayslip, and R. N. Hoy 1978. Electrical conductivity and relaxation in ice crystals with known impurity content. *J. Glaciol*. **21**, 143–159.

Gross, G. W., P. M. Wong, and K. Humes 1977. Concentration-dependent solute redistribution at the ice–water phase boundary, III. Spontaneous convection: Chloride solutions. *J. Chem. Phys*. **67**, 5264–5274.

Kargel, J. S. 1991. Brine volcanism and the interior structures of asteroids and icy satellites. *Icarus* **94**, 368–390.

Kargel, J. S. 1996. Europa's crust and ocean: Origin, composition, and possible implications for Io's early conditions (abstract), Europa Ocean Conference, Capistrano Conference No. 5. San Juan Capistrano Institute, CA.

Khurana, K. K., M. G Kivelson, D. J. Stevenson, G. Schubert, C. T. Russell, R. J. Walker, S. Joy, and C. Polanskey 1998. Oceans in Europa and Callisto: Independent evidence from magnetic perturbations. *Nature* **395**, 777–780.

Kovacs, A., R. M. Morey, and G. F. N. Cox 1987. Modeling the electromagnetic property trends in sea ice, part 1. *Cold Reg. Sci. Technol.* **14**, 207–235.

Lorenz, R. D. 1998. Preliminary measurements of the cryogenic dielectric properties of water–ammonia ices: Implications for radar observations of icy satellites. *Icarus* **136**, 344–348.

McCord, T. B., G. B. Hansen, F. P. Fanale, R. W. Carlson, D. L. Matson, T. V. Johnson, W. D. Smythe, J. K. Crowley, P. D. Martin, A. Ocampo, C. A. Hibbitts, J. C. Granahan, and the NIMS Team 1998. Salts on Europa's surface detected by Galileo's near infrared mapping spectrometer. *Science* **280**, 1242–1245.

McKinnon, W. B. 1999. Convective instability in Europa's ice shell. *Geophys. Res. Lett.* **26**, 951–954.

Moore, J. C., and S. Fujita 1993. Dielectric properties of ice containing acid and salt impurities at microwave and LF frequencies. *J. Geophys. Res*. **98**, 9769–9780.

Moore, J. C., J. G. Paren, and H. Oerter 1992. Sea salt dependent electrical conduction in polar ice. *J. Geophys. Res*. **97**, 19803–19812.

Moore, J. C., A. P. Reid, and J. Kipfstuhl 1994. Microphysical and electrical properties of marine ice and its relationship to meteoric and sea ice. *J. Geophys. Res*. **99**, 5171–5180.

Oerter, H., J. Kipfstuhl, J. Determann, H. Millar, D. Wagenbach, A. S. A. Minikin, and W. Graf 1992. Evidence for basal marine ice in the Filchner–Ronne Ice Shelf. *Nature* **358**, 399–401.

Ojakangas, G. W., and D. J. Stevenson 1989. Thermal state of an ice shell on Europa. *Icarus* **81**, 220–241.

Pappalardo, R. T., J. W. Head, R. Greeley, R. J. Sullivan, C. Pilcher, G. Schubert, W. B. Moore, M. H. Carr, J. M. Moore, M. J. S. Belton, and D. L. Goldsby 1998. Geological evidence for solid-state convection in Europa's ice shell. *Nature* **391**, 365–368.

Squyres, S. W., R. T. Reynolds, P. M. Cassen, and S. J. Peale 1983. Liquid water and active resurfacing on Europa. *Nature* **301**, 225–226.

Weeks, W. F., A. J. Gow, P. Kosloff, and S. Digby-Argus 1990. The internal structure, composition and properties of brackish ice from the Bay of Bothnia. In *Sea Ice Properties and Processes* (S. F. Ackley and W. F. Weeks, Eds.), CRREL Monograph. 90-1, pp. 5–15. Cold Regions Research and Engineering Laboratory, Hanover, New Mexico.

Wolff, E. W., W. D. Miners, J. C. Moore, and J. G. Paren 1997. Factors controlling the electrical conductivity of ice from the Polar regions—A summary. *J. Phys. Chem*. **101**, 6090–6094.